Surface formation routes of interstellar molecules : a laboratory study
Sergio, I.

CHAPTER 3

Laboratory Evidence for Efficient Water Formation in Interstellar Ices [1]

Even though water is the main constituent in interstellar icy mantles, its chemical origin is not well understood. Three different formation routes have been proposed following hydrogenation of O, O_2, or O_3, but experimental evidence is largely lacking. We present a solid state astrochemical laboratory study in which one of these routes is tested. For this purpose O_2 ice is bombarded by H- or D-atoms under ultra high vacuum conditions at astronomically relevant temperatures ranging from 12 to 28 K. The use of reflection absorption infrared spectroscopy (RAIRS) permits derivation of reaction rates and shows efficient formation of H_2O (D_2O) with a rate that is surprisingly independent of temperature. This formation route converts O_2 into H_2O via H_2O_2 and is found to be orders of magnitude more efficient than previously assumed. It should therefore be considered as an important channel for interstellar water ice formation as illustrated by astrochemical model calculations.

3.1   Introduction

Solid water ice has been observed on the surfaces of many different astronomical objects. In the Solar System it is found on planets and minor bodies such as comets, trans-Neptunian objects and Centaurs. In dense, cold interstellar clouds, infrared observations show that interstellar dust grains are covered with water-rich ices (*e.g.,* Gillett & Forrest 1973, Gibb et al. 2004, Pontoppidan et al. 2004). The formation of these ice mantles is especially important in the process of star and planet formation, when a large fraction of heavy elements can be depleted onto grains. In the dense cloud phase water layers form on the bare grain surfaces. Then during the gravitational (pre-)collapse, virtually all gas phase species freeze-out on top of these water layers resulting in a CO dominated layer that likely also contains traces of O_2 but very little water.

The observed H_2O ice abundance cannot be explained by direct accretion from the gas phase only. The exact mechanism by which water ice is formed is not understood. The *Herschel Space Observatory*, to be launched in the near future, will provide important new information on gaseous water in interstellar space and will measure quantitatively the water abundance as a function of temperature, UV field and other parameters. Furthermore, the *Photodetector Array Camera and Spectrometer* (PACS) on *Herschel* will cover the 62 μm band of solid H_2O. In this way *Herschel* will provide a unique opportunity to observe the bulk of the water bands that are unobservable from the ground and relate them to *Spitzer* and groundbased mid-IR observations of ices in protostellar envelopes and protoplanetary disks. Understanding the processes by which water forms and why it is not formed under other circumstances will be essential for the interpretation of these data.

Tielens & Hagen (1982) proposed a reaction scheme in which water ice is formed on the surfaces of grains via three different routes: hydrogenation of O, O_2, and O_3. Models predict that water can indeed be formed through such reactions in dense clouds (e.g., Tielens & Hagen 1982, d'Hendecourt et al. 1985, Hasegawa & Herbst 1993, Cuppen & Herbst 2007). Using a Monte Carlo approach Cuppen & Herbst (2007) showed that the contributions of the different formation channels to water ice formation as well as its abundance strongly depend on the local environment. However, the initial reaction scheme with the corresponding rates as proposed by Tielens & Hagen (1982) is based on old, in some cases outdated, gas phase data of the equivalent reactions. Progress has been severely hampered by the lack of realistic experimental simulations of these low-temperature, solid state reactions. Preliminary laboratory studies of water synthesis testing the first reaction channel have been reported by Hiraoka et al. (1998) and by Dulieu et al. (2007). Both groups investigated the products of D- and O- reactions on an ice substrate (N_2O and H_2O, respectively) using temperature programmed desorption (TPD). In experiments exclusively using this technique, it is hard to rule out any H_2O formation during warm up. Furthermore, quantitative interpretation can be tricky because unstable species like H_2O_2 are destroyed in the mass spectrometer upon ionization leading to an artificially enhanced H_2O/H_2O_2 ratio. This chapter focuses on the H + O_2 channel in

which O_2 is converted to H_2O via H_2O_2:

$$H + O_2 \rightarrow HO_2 \tag{3.1}$$

$$H + HO_2 \rightarrow H_2O_2 \tag{3.2}$$

$$H + H_2O_2 \rightarrow H_2O + OH \tag{3.3}$$

$$H + OH \rightarrow H_2O \tag{3.4}$$

According to Cuppen & Herbst (2007) this channel is, together with the O_3 channel, responsible for water formation in cold, dense clouds. The exposure of O_2 ice to hydrogen and deuterium atoms is investigated by means of reflection absorption infrared spectroscopy (RAIRS) and TPD. These techniques allow one to determine formation yields and the corresponding reaction rates. The present chapter comprises a study of hydrogenation and deuteration reactions of O_2 ice for different temperatures between 12 and 28 K, *i.e.*, up to the desorption temperature of O_2 (Acharyya et al. 2007). The formation of H_2O and H_2O_2 is observed at all temperatures. An optimum yield is found at 28 K.

3.2 Experiment

Experiments are performed using an ultra-high vacuum set-up ($<5 \times 10^{-10}$ mbar) which comprises a main chamber and an atomic line unit. The set-up is discussed in more detail in Fuchs et al. (2009). The main chamber contains a gold coated copper substrate (2.5×2.5 cm^2) that is in thermal contact with the cold finger of a 12 K He cryostat. The temperature can be varied with 0.5 K precision between 12 and 300 K. A precision leak valve is used to deposit O_2 (99.999% purity, Praxair) on the substrate. Ices are grown at 45° with a flow of 1×10^{-7} mbar s^{-1} where 1.3×10^{-6} mbar s^{-1} corresponds to 1 Langmuir (L) s^{-1}. In order to compare results from different experiments, the thickness of the O_2 ice is 75 L for all samples studied and the substrate temperature is kept at 15 K during the deposition. An O_2 ice of 75 L consists of roughly 30 monolayers. This thickness is chosen to exclude substrate induced effects. Because a diatomic homonuclear molecule like O_2 is infrared in-active, gas phase O_2 is monitored during the deposition by a quadrupole mass spectrometer (QMS). After deposition at 15 K the ice is slowly cooled down or heated (1 K min^{-1}) until a selected temperature is reached. Systematic studies are performed for different temperatures between 12 and 28 K.

H(D)-atoms are produced in a well-characterized thermal-cracking device (Tschersich & von Bonin 1998, Tschersich 2000). A second precision leak valve is used to admit H_2 (D_2) molecules (99.8% purity, Praxair) into the gas cracking line. In each experiment the H + H_2 (D + D_2) flow through the capillary in the atomic line is 1×10^{-5} mbar s^{-1} and the temperature of the heated tungsten filament, which surrounds the gas cracking pipe, is about 2300 K. The dissociation rate and the atomic flux depend on the pressure and temperature (Tschersich 2000) and are kept constant during all the experiments. A nose-shaped quartz pipe is placed along the path of the atomic beam in order to cool down H(D)-atoms to room temperature before reaching the ice sample by collisions (Walraven

& Silvera 1982). The H(D)-atomic flux nearby the sample is estimated, within 50%, as 5×10^{13} cm^{-2} s^{-1}. At temperatures of 12 K and higher, no blocking of surface processes by the presence of H_2 is expected in the ice.

The newly formed species after hydrogenation (deuteration) of O_2 ice are monitored by RAIRS using a Fourier transform infrared spectrometer (FTIR) running at a spectral resolution of 4 cm^{-1} in the range between 4000 and 700 cm^{-1} (2.5−14 μm). Typically the ice is exposed to the H (or D) beam for 3 (or 2) hours and IR spectra are acquired every few minutes.

Systematic control experiments have been performed in order *(i)* to unambiguously confirm that the products are formed by surface processes and not by gas phase reactions, *(ii)* to check that any water present in the system does not affect the final results and *(iii)* to verify that water and H_2O_2 formation occurs in the solid phase after H(D)-atom bombardment and not by $H_2(D_2)$-molecules addition. For *(i)* co-deposition experiments are undertaken in which H and O_2 are deposited simultaneously. Water is only formed if the surface temperature is below the desorption temperature of oxygen, confirming that the presence of the oxygen ice is required for this reaction sequence to occur. Point *(ii)* is verified by using inert initial substrates like N_2 ice to estimate the background water contribution, as well as by using different isotopologues ($^{18}O_2$, $^{15}N_2$ and D). Finally *(iii)* is checked by using pure $H_2(D_2)$-beams, *i.e.*, without any H(D) present.

3.3 Results

The formation of both H_2O_2 and H_2O ice is confirmed by the appearance of their infrared solid state spectral signatures. Figure 3.1 shows typical RAIRS results for hydrogenation and deuteration of O_2 ice at 25 K. From top to bottom a time sequence of four spectra is plotted. These spectra are difference spectra with respect to the initial oxygen ice. However, since our initial oxygen ice only consists of 30 ML, no features due to the intrinsically very weak O_2 feature (Ehrenfreund et al. 1992, Bennett & Kaiser 2005) are observed in the original spectrum. Both the H_2O and H_2O_2 clearly grow in time as the H-fluence (H-flux × time) increases. Similar features appear for the deuteration experiment, although here clearly less D_2O is formed. After fitting the infrared spectra with a straight baseline the column density (molecules cm^{-2}) of the newly formed species in the ice is calculated from the integrated intensity of the infrared bands using a modified Lambert-Beers equation (Bennett et al. 2004). In the range of our spectrometer, water ice has two candidate bands for determining its column density, at 3430 cm^{-1} and 1650 cm^{-1} (3 and 6 μm, respectively). Since the strong 3430 cm^{-1} feature overlaps with the 3250 cm^{-1} band of H_2O_2, the weak feature at 1650 cm^{-1} was chosen to quantify the water column density. Since literature values of transmission band strengths cannot be used in reflection measurements, an apparent absorption strength is obtained from a calibration experiment in which a pure water ice layer desorbs at constant temperature until the sub-monolayer regime (Öberg et al. 2007b). The uncertainty in the band strengths remains within a factor of two. Quantification of H_2O_2 is done using the 1350 cm^{-1} band. As it is experimentally very hard to deposit pure H_2O_2 ice, the apparent absorption strength has to be obtained

indirectly by assuming the ratio of the integrated band strengths between the two bands in transmittance to be the same as in reflectance $H_2O/H_2O_2 = 0.57$ (Gerakines et al. 1995, Loeffler et al. 2006). The band modes of solid D_2O and D_2O_2 ices have systematic peak position shifts of ~400 cm^{-1} with respect to the H_2O and H_2O_2 bands. The column density for deuterated species is obtained in a similar way from a calibration experiment, while the absorption strength for D_2O_2 is estimated assuming that $H_2O/H_2O_2 = D_2O/D_2O_2$.

In Fig. 3.2 the column densities of water and H_2O_2 are plotted as a function of the H(D)-fluence (atoms cm^{-2}) for different substrate temperatures. The results for H_2O_2 and D_2O_2 are found to be very reproducible (errors within the symbols). Due to their low column densities the relative errors for H_2O and especially D_2O are larger. The H_2O_2 and D_2O_2 results all show the same initial linear increase followed by a very sharp transition to a steady state column density, with the steady state value increasing with temperature. The water results show similar behavior although the transition is not as sharp and the temperature dependence of the steady-state value is not as clear. The observation that the results for all temperatures show the same initial slope means that the rate of the reaction to H_2O_2 is temperature independent. The final yield is however temperature dependent and this depends on the penetration depth of the hydrogen atoms into the O_2 ices; at higher temperatures H-atoms can penetrate deeper. This is discussed in more detail later.

During the preparation of this manuscript we received a preprint by Miyauchi et al. (2008) who performed a similar experiment for one single temperature (10 K). Our results for 12 K turn out to be close to their results, apart from an absolute scaling due to different assumptions on the band strengths.

3.4   Determining the reaction rates

Reaction rates are obtained by fitting a set of differential equations to the time evolution curves of H_2O (D_2O) and H_2O_2 (D_2O_2). Usually a diffusive mechanism is considered to construct these equations. For H_2O_2 that is formed from oxygen and converted into water as given in Eqs. 3.1-3.4 the rate equation would be

$$\frac{dn_{H_2O_2}(t)}{dt} = (k_{hop}^H + k_{hop}^{O_2})k_1 n_H(t) n_{O_2}(t)$$
$$- (k_{hop}^H + k_{hop}^{H_2O_2})k_3 n_H(t) n_{H_2O_2}(t) \tag{3.5}$$

with k_{hop}^X and n_X the hopping rate and column density of species X and k_1 and k_3 the rate constants of reactions (3.1) and (3.3).

Awad et al. (2005) and Miyauchi et al. (2008) applied similar expressions to determine the rates of the formation of methanol and water, respectively. They solved these equations under the assumption that the atomic hydrogen abundance on the surface remains constant. In this way expressions for the surface abundances of the reaction products were obtained with only the effective reaction rates as fitting parameter

$$n_{H_2O_2} = n_{O_2}(0)\frac{\beta_1}{\beta_1 - \beta_3}\left(\exp(-\beta_3 t) - \exp(-\beta_1 t)\right), \tag{3.6}$$

with

$$\beta_1 = (k_{\text{hop}}^{\text{H}} + k_{\text{hop}}^{\text{O}_2})k_1 n_{\text{H}}. \tag{3.7}$$

Fitting this expression to the experimental data points in Fig. 3.2 gives a very poor agreement because the model has an exponential behavior whereas the experiments for several temperature values clearly do not. This would moreover result in a different rate for H + O$_2$ for each temperature whereas the experimental curves show that the rate is independent of temperature. For this reason we decided to use a different model. We consider two regimes. In the first regime ($t < t_t$) the hydrogen atoms get trapped into the ice with an efficiency that is independent of temperature. Once an atom is trapped it can diffuse efficiently and find an oxygen molecule to react with. This results in a zeroth order rate. Once nearly all oxygen molecules within the penetration depth are converted to H$_2$O$_2$ ($t > t_t$), diffusion becomes rate limiting and a diffusive mechanism for the reaction to H$_2$O$_2$ and H$_2$O is applied. Since now the ice is changed from an O$_2$ ice to an H$_2$O$_2$ ice the penetration depth of the H-atoms into the ice will change as well. This model is described by the following set of equations

$$n_{\text{H}_2\text{O}_2} = \beta_1' t \frac{p_{\text{O}_2} - p_{\text{H}_2\text{O}_2}}{p_{\text{O}_2}} + \frac{\beta_1'}{\beta_3} \frac{p_{\text{H}_2\text{O}_2}}{p_{\text{O}_2}} (1 - \exp(-\beta_3 t)) \tag{3.8}$$

$$n_{\text{H}_2\text{O}} = \beta_1' \frac{p_{\text{H}_2\text{O}_2}}{p_{\text{O}_2}} \left(t - \frac{1 - \exp(-\beta_3 t)}{\beta_3} \right) \tag{3.9}$$

for $t < t_t$ and

$$\begin{aligned} n_{\text{H}_2\text{O}_2} = & \frac{\beta_1'}{\beta_3} \frac{p_{\text{H}_2\text{O}_2}}{p_{\text{O}_2}} \exp(-\beta_3 t) \left(\exp(\beta_3 t_t) - 1 \right) \\ & + \frac{n_{\text{O}_2}(t_t)}{\beta_3 - \beta_1} \frac{p_{\text{H}_2\text{O}_2}}{p_{\text{O}_2}} (\beta_1 \exp(-\beta_3(t - t_t)) - \beta_3 \exp(-\beta_1(t - t_t))) \\ & - n_{\text{O}_2} - p_{\text{H}_2\text{O}_2} + p_{\text{O}_2} \end{aligned} \tag{3.10}$$

$$\begin{aligned} n_{\text{H}_2\text{O}} = & -\frac{\beta_1'}{\beta_3} \frac{p_{\text{H}_2\text{O}_2}}{p_{\text{O}_2}} \exp(-\beta_3 t) \left(\exp(\beta_3 t_t) - 1 \right) \\ & - \frac{n_{\text{O}_2}(t_t)}{\beta_3 - \beta_1} \frac{p_{\text{H}_2\text{O}_2}}{p_{\text{O}_2}} (\beta_1 \exp(-\beta_3(t - t_t)) - \beta_3 \exp(-\beta_1(t - t_t))) \\ & + p_{\text{H}_2\text{O}_2} \end{aligned} \tag{3.11}$$

for $t > t_t$ with p_{X} the penetration depth of H-atoms into ice X in units of column density, β_1 and β_1' the effective rates of reaction (3.1) and β_3 the rate of reaction (3.3). β_1 and β_3 represent effective diffusive rates that include both the diffusion rate and the reaction rate, whereas β_1' is mainly determined by the hydrogen flux times the efficiency of H trapping into the ice.
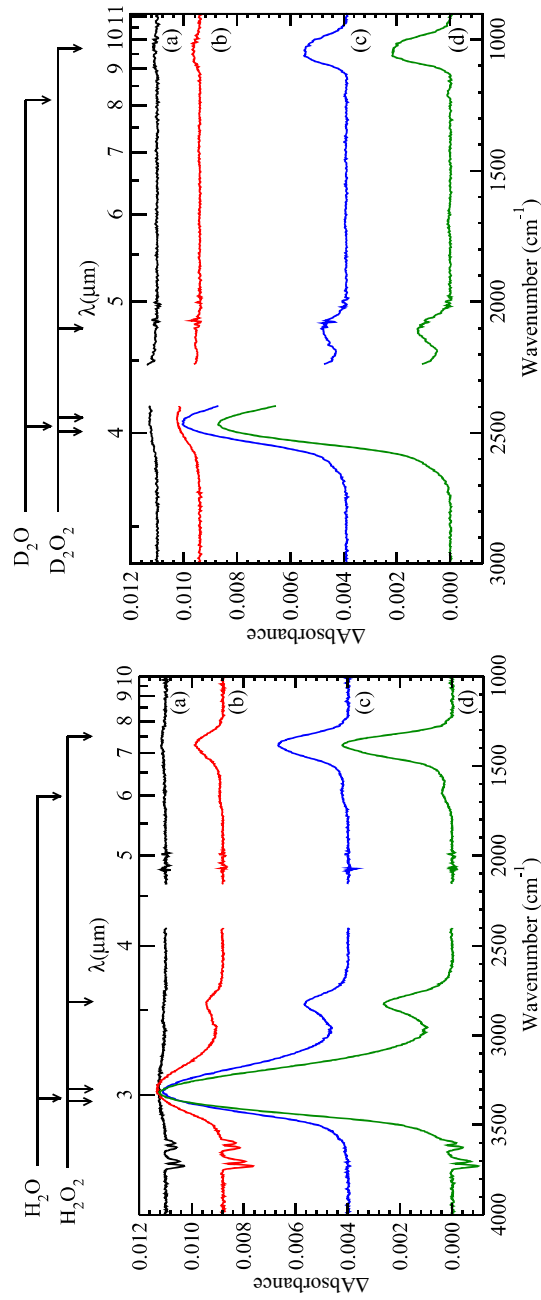
Figure 3.1 RAIR spectral changes of the O_2 ice as a function of H-atom (*left*) and D-atom (*right*) bombardment at 25 K. Spectra at a H(D)-atom fluence of (a) 4×10^{15}, (b) 4×10^{16}, (c) 1×10^{17}, and (d) 2×10^{17} cm^{-2} are given.
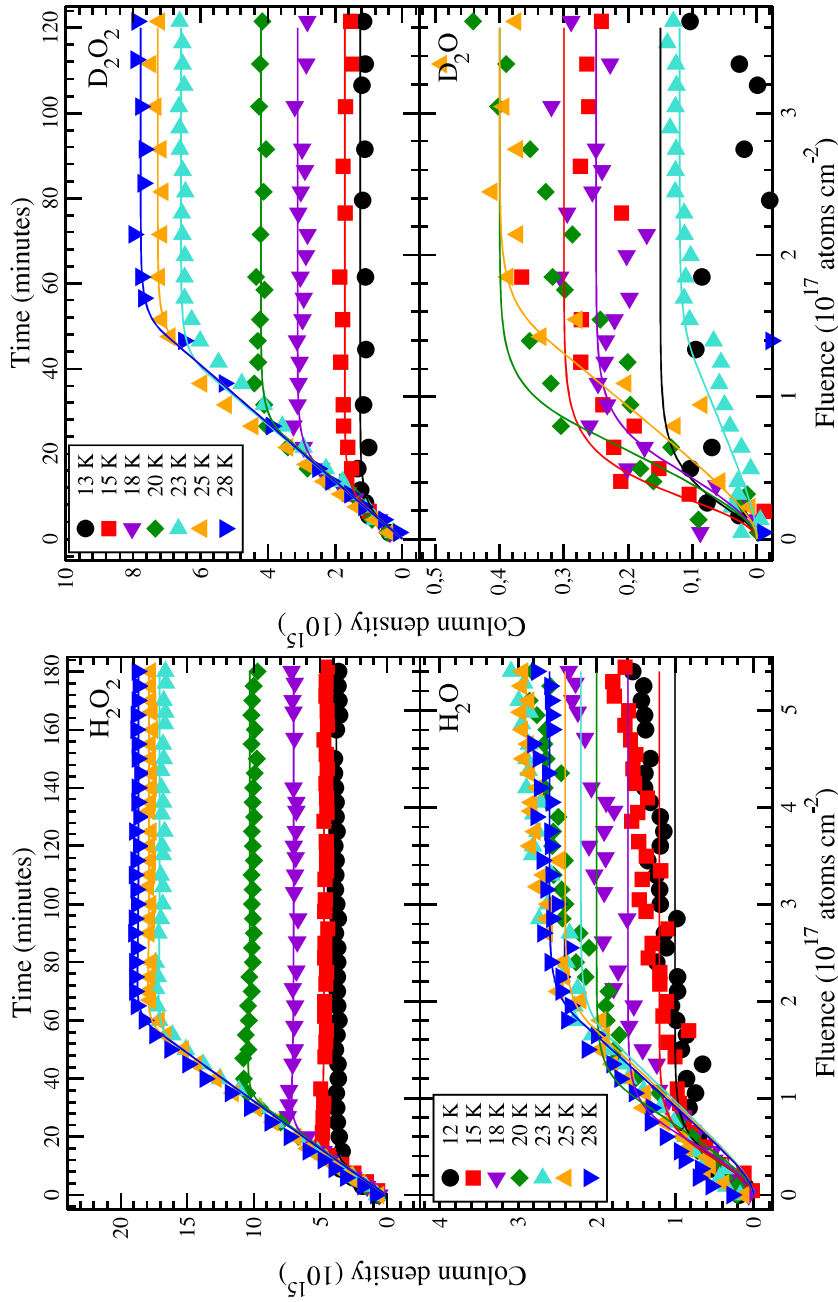
Figure 3.2 The column densities of H_2O_2/D_2O_2 (*top*) and H_2O/D_2O (*bottom*) as a function of time and fluence for different surface temperatures. The symbols indicate experimental data, the solid lines represent the fitted model. The left panel is for hydrogenation, the right for deuteration.

Fitting this model to the data, the three rates are found to be independent of temperature. We therefore apply the same average rate to describe the results at all temperatures and only the two penetration depths are allowed to vary between the experiments. The resulting curves are indicated by the solid lines in Fig. 3.2. The obtained rates are given in Table 3.1. The penetration depths are the steady state values in Fig. 3.2. These clearly increase with temperature to very high values. This suggests that as the O_2 ice reaches its desorption temperature (~30 K) the structure becomes more open and the O_2 molecules more mobile, allowing the hydrogen atoms to penetrate deeply into the ice. The H_2O_2 structure on the contrary is much more dense and rigid and consequently the H(D)-atoms cannot penetrate more than a few monolayers even at the highest temperatures. The temperature effect is also much less prominent in cases where the ice is comfortably below its desorption temperature.

Table 3.1 The reaction rates obtained by fitting the model. For the corresponding uncertainties see the text.

	β_1' [molec cm^{-2}s^{-1}]	β_1 [s^{-1}]	β_3 [s^{-1}]
H + O_2	5.4×10^{12}	3.3×10^{-3}	2.7×10^{-3}
D + O_2	2.5×10^{12}	3.3×10^{-3}	2.7×10^{-3}

A clear difference in penetration depth between the hydrogenation and deuteration experiments can be observed. For the oxygen penetration depth a difference of a factor of two is found whereas for hydrogen and deuterium peroxide the difference can be even as high as a factor of six.

Like in the models by Awad et al. (2005) and Miyauchi et al. (2008), the rates β_1 and β_3 are the products between the rates of the reactions and the hydrogen surface abundance. The latter is assumed to be constant during the experiment and is the overall result of accretion, desorption and reaction with both H and O_2. A comparison of β_1' and β_1 indicates that the reaction with H only plays a minor role.

The uncertainties in β_1 and β_3 are mainly determined by the fit and are within 50%. The error in β_1' due to the fit is much less, but here the main uncertainty is determined by the layer thickness. The error in the calibration of the layer thickness is a factor of two. Assuming that every hydrogen atom that gets trapped reacts with O_2 and considering that two hydrogen atoms are needed to convert O_2 to H_2O_2, the trapping efficiency can be determined from β_1' and the flux (5×10^{13} cm^{-2} s^{-1}). This results in a trapping efficiency of ~10% for deuterium and ~20% for atomic hydrogen. This is very close to the sticking efficiency of hydrogen atoms to a water ice surface of ~30% under these circumstances (Al-Halabi & van Dishoeck 2007). The high efficiency of reaction (3.1) is consistent with recent theoretical studies of this reaction in the gas phase. Xie et al. (2007) and Xu et al. (2005) found that this reaction can proceed barrierless for certain incoming angles. The rates β_1 and β_3 have very similar values. This suggests that also reaction (3.3) is very efficient and H_2O formation is only limited by the penetration depth of H_2O_2.

The rate of reaction (3.3) shows no significant isotope effect. This is in contrast with the results by Miyauchi et al. (2008) who found a significant isotope effect for this reaction using the diffusive model to fit their 10 K results. If a large barrier is involved in reaction (3.3), barrier crossing would proceed via tunneling and an isotope effect is expected (Watanabe, private communications). The fact that we do not observe a (large) effect at 12−28 K either suggests that the barrier for this reaction is low or that other mechanisms for the formation of water should be taken into account in the model to fit the data. We will address this question in Chapters 4 and 5. For now the conclusion remains that the formation of water from O_2 and H is very efficient.

3.5   Astrophysical discussion and conclusion

The hydrogenation and deuteration experiments presented in this letter show an efficient mechanism to convert O_2 ice to H_2O_2 and ultimately H_2O. In the model that describes these experiments, the rate limiting steps for formation are the trapping of the hydrogen into the O_2 ice and the penetration depth of the hydrogen into the H_2O_2. Astrochemical models take reaction, diffusion and desorption barriers as input. Our data shows that the formation of at least H_2O_2 proceeds via a reaction with a barrier that is much lower than the value of 1200 K previously assumed by Tielens & Hagen (1982). It should therefore be considered as a route for water formation on interstellar grain surfaces.

Care should however be taken when extending these findings from a laboratory environment directly to interstellar ices. The temperature independence of the reaction rate that is observed, for instance, is directly due to the unique property of the O_2 ice that allows hydrogen to penetrate its structure and thereby preventing desorption back into the gas phase. In interstellar clouds the mantle surfaces would not consist of pure O_2 ice but of a mixture of different species with water as its main constituent (Whittet et al. 1998). The structure of these "dirty" ices and the binding energies to it would govern the desorption and diffusion behavior of adsorbates like O_2 and H. Experiments on the binding of atomic hydrogen on water ice surfaces showed that the surface abundance is generally dependent on temperature (Perets et al. 2005, Hornekær et al. 2003, Dulieu et al. 2005). Also hydrogenation experiments of CO showed that the decreasing H coverage for increasing temperature results in lower effective rates (Watanabe et al. 2003, 2006b, Linnartz et al. 2007, Cuppen et al. 2008). Here we discuss the implications of the present work to two different interstellar environments: hydrogenation of an apolar (water-poor) ice mantle after freeze-out and cold cloud conditions where ice is formed from direct deposition of H and O.

Observations show that interstellar ice mantles consist of polar (water-rich) and apolar (water-poor) layers Tielens et al. (1991). Apolar ices are thought to form during freeze-out in the densest parts of the cloud. In dense gas, most of the atomic oxygen has converted to O_2 which can become subsequently a constituent of this polar phase. The lack of observed H_2O_2 and H_2O means that most of the O_2 in the ice does not react to produce H_2O_2 or H_2O. This laboratory work however shows that hydrogen atoms can penetrate deeply into O_2 ices and then react. In apolar interstellar ices the penetration depth is not
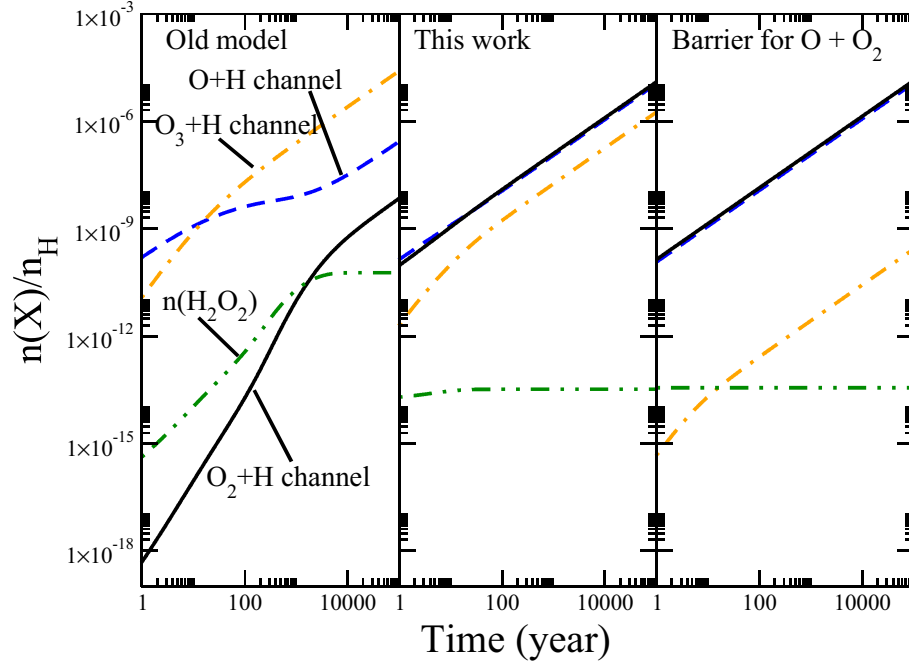
Figure 3.3 The contributions of the three different channels to H_2O formation in three models and the H_2O_2 abundance, $n(H_2O_2)$ from the $O_2 + H$ channel. (*left*) Old network by Tielens & Hagen (1982), (*middle*) new network without barriers for reactions (3.1) and (3.3) and (*right*) new network with barrier for $O + O_2$ reaction. See text for details.

determined by oxygen ice but by the main constituent of the ice mantle, CO. We therefore have performed additional laboratory experiments in which a mixture of CO and O_2 ice is exposed to H-atoms. These show indeed that only the top few layers are hydrogenated and that the main part of the ice stays intact in agreement with the observations. Details of these experiments are reported in Ioppolo et al. (2010b) (Chapter 7).

In cold and translucent clouds H- and O-atoms deposit onto the grain simultaneously. The species can then react immediately and O_2 is converted all the way to water. Here the penetration depth observed in the laboratory becomes unimportant. What can we learn from the present experiments then? The fast reaction kinetics justify treating $H + O_2$ and $H + HO_2$ in a similar way as $H + H$ are treated in astrochemical models, with the difference that probably only hydrogen is mobile for reaction. The results further suggest that the continuing reactions leading to water proceed with high efficiency. The original grain surface network by (Tielens & Hagen 1982) includes two more water formation routes: via OH and via ozone. Under dense cloud conditions the ozone route was proposed to be the most efficient as is shown in the left panel of Fig. 3.3. This figure plots the contributions for the three different H_2O formation channels using a reaction network

limited to the three water formation routes and without any dissociation reactions. The model parameters are taken from model M1 by Ruffle & Herbst (2000) and the initial conditions from Tielens & Hagen (1982) are used ($n(H_2) = 5 \times 10^4$, $n(H) = 1.41$ and $n(O) = 2.36$ cm^{-2}). These calculations include a barrier for reactions (3.1) and (3.3). The present work shows that these barriers are negligible and the middle panel plots the same model calculation without these barriers. The figure clearly shows that the O_2 channel has a major contribution to the overall water formation rate. Recent laboratory experiments by Sivaraman et al. (2007) on the temperature-dependent formation of ozone by irradiation of oxygen ices by high energy electrons suggest that mobile oxygen atoms prefer the O + O pathway over O + O_2 even though the O/O_2 ratio in the ice is very small. This implies the presence of a barrier for the formation of ozone. The right panel gives the model results when a small barrier of 500 K for this reaction is considered. The contribution of the ozone channel is now further reduced.

Figure 3.3 further shows the H_2O_2 abundance, $n(H_2O_2)$, for all models as produced through the O_2 + H route. Boudin et al. (1998) set an observational constraint of the H_2O_2 ice abundance toward NGC 7538 IRS9 of 5.2% with respect to the H_2O ice abundance. All models are consistent with this number.